Contributions of Dipolar Relaxation Processes and Ionic Transport to the Response of Liquids to Electrical Perturbation Fields

7 AUTHORS, INCLUDING:

M.J. Sanchis
Universitat Politècnica de València
106 PUBLICATIONS **869** CITATIONS

SEE PROFILE

Pilar Ortiz-Serna
Universitat Politècnica de València
17 PUBLICATIONS **51** CITATIONS

SEE PROFILE

Ricardo Díaz-Calleja
Universitat Politècnica de València
223 PUBLICATIONS **1,720** CITATIONS

SEE PROFILE

Ligia Gargallo
University of Tarapacá
282 PUBLICATIONS **1,850** CITATIONS

SEE PROFILE

Contributions of Dipolar Relaxation Processes and Ionic Transport to the Response of Liquids to Electrical Perturbation Fields

M. J. Sanchis, P. Ortiz-Serna, M. Carsí, and R. Díaz-Calleja*

Instituto Tecnológico de la Energía (ITE), Universitat Politècnica de València, Spain

E. Riande*

Instituto de Ciencia y Tecnología de Polímeros (CSIC), Juan de la Cierva 3, 28006 Madrid, Spain

L. Gargallo and D. Radić

Departamento de Química Física, Pontificia Universidad Católica de Chile, Santiago, Chile

Ⓢ Supporting Information

ABSTRACT: The objective of this work was to study the influence of small variations in the chemical structure on the molecular dynamics of liquids using as models bis(cyclohexylmethyl) 2-methyl- and dicyclohexyl 2-methylsuccinate. The dielectric behavior of the low molecular weight liquids was studied over a wide range of frequencies and temperatures. The results show that the temperature dependence of the dielectric strengths, relaxation times, and shape parameters of the secondary and glass—liquid relaxations are very sensitive to the slight differences in the structures of the liquids. Significant changes take place in the dielectric strength of the β relaxation in the glass liquid transition. Moreover, the temperature dependence of the β relaxation exhibits Arrhenius behavior in the glassy state and departs from this behavior in the liquid state. Special attention is paid to the temperature dependence of low-frequency relaxations produced by the motion of a macrodipole arising from charges located near the liquid—electrode boundaries.
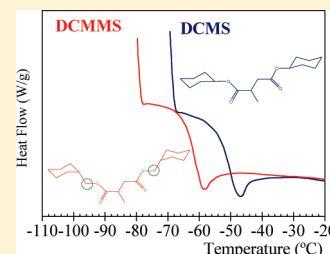
■ INTRODUCTION

Traditionally, the study of the response of supercooled liquids to perturbation fields has fascinated scientists with research interests focused on the physics of condensed matter. This is so because an understanding of the dynamics of supercooled liquids is paramount to explain the physics involved in the glass transition, one of the most important unsolved subjects in the physics of condensed matter.[1−6]

In cooling, supercooled liquids may reach a temperature in the vicinity of which ergodicity is lost.[1] The relaxation time associated with the response in this case, τ_α, undergoes an anomalous increase as temperature decreases due to the increase of co-operativity for diffusive displacement caused by less volume available,[1] this latter parameter being dependent on pressure and temperature.[7] The glass transition temperature T_g can be defined as that at which the relaxation time of the system is larger than the time scale of the experiment. Above T_g the material is a liquid, below a glass. Since the glass transition is a kinetic phenomenon, i.e., depends on the cooling rate, some authors consider T_g the temperature at which the relaxation time of the system is larger than 200 s.[1] The glass transition is closely related to the molecular mobility, and as a result monomers exhibit lower glass transition temperatures than polymers. In spite of this, the dynamics of monomers and polymers are similar in the sense that the response of liquids to perturbation fields, at the moderately

supercooled level, is a single relaxation. However, in cooling a temperature is reached at which the relaxation splits into a fast process called β relaxation and a slow one called glass—liquid or α relaxation.[8−10] On decreasing the temperature even further, the α relaxation shifts to lower frequencies more rapidly than the β relaxation, and the distance between the peaks of the two absorptions increases as the temperature decreases. At T_g, cooperative motions producing the α relaxation freeze-in, but the β absorption remains operative below T_g. The glass—liquid relaxation is the precursor of the liquid state, and the understanding of the glass transition will require a good knowledge of the chemical structure effect on the α relaxation. The dynamics of glass-forming systems can only be defined if T and p are specified. The effect of pressure on the α and β processes is different in the sense that this thermodynamic variable exerts a stronger influence on the glass—liquid relaxation than on the faster or secondary relaxation processes. Therefore, by combining pressure and temperature, the deconvolution of overlapped primary and secondary relaxations is facilitated.[7,9]

Although the secondary β process is considered to arise from motions of only a part of the molecule, the fact that the spectra of

low molecular weight rigid molecules, such as bromobenzene, exhibit the β absorption suggests that the development of this process in these cases entails the motion of the entire molecule as a whole.[11,12] This type of relaxation characteristic of rigid glass formers and perhaps of all glass formers is often named Johari−Goldstein (JG) β relaxation. Although in the current literature β processes are in many cases indistinctly named JG β relaxations, a criterion commonly invoked is the tendency of the β relaxation to merge with the glass−liquid relaxation.[10,13] Pursuing this line of research, this work studies how small changes in the chemical structure of low molecular weight compounds or monomers influence the dielectric relaxation behavior. As models bis(cyclohexylmethyl) 2-methylsuccinate (DCMMS) and dicyclohexyl 2-methylsuccinate (DCMS) were used. The molecular structures of these compounds, shown in Figure 1, present permanent dipoles of 1.78 D associated with each ester group which form an angle of 143° with the $CH_2-C(O)O$ bond.[14] The dielectric α relaxation presumably arises from cooperative motions of molecules, whereas internal motions of the backbone in a variety of environments produce the β process. With increasing temperature, the concert of the overall motions of the molecular backbone produces the merging or coalescence of the α and β relaxations, forming the $\alpha\beta$ process. The α process relaxes the fraction of mean-square dipole moment remaining after the β process takes place.[7,10,13]

One of the aims of this work was to study the effect of slight modifications in chemical structure on the relaxation strengths of the α and β relaxations and on the temperature dependence of the relaxation times associated with both processes. The closeness of the chemical structure of the two methyl succinate compounds used in this work allows the fulfillment of this objective. On the other hand, traces of water and other impurities strongly affect the components of the complex permittivity of real systems at low frequencies. However, since most dielectric studies are focused on the dipolar relaxation behavior, the changes observed in the real and loss components of the complex permittivity in the low-frequency region are in most cases ignored. In this work special attention is paid to the contribution of the ionic transport to the dielectric responses of the systems to electric perturbation fields in the low-frequency region where the contribution of dipolar processes to the permittivity is negligible.

■ EXPERIMENTAL SECTION

DCMMS and DCMS were synthesized by esterification of 2-methylsuccinic acid with (hydroxymethyl)cyclohexane and cyclohexanol, respectively, using toluene-4-sulfonic acid as the catalyst. Briefly, 1 mol of acid and 2 mol of alcohol with a 5% excess of alcohol were refluxed in toluene for 4 h in a Dean−Stark three-necked flask to remove the water produced in the esterification process. The reaction product was dried with magnesium sulfate and further distilled under vacuum (1 mmHg). Products were characterized by FT-IR and ^1H NMR, and the signals obtained correspond to the expected chemical structure. The respective glass transition temperatures of DCMMS and DCMS were measured with a differential scanning calorimeter (Perkin-Elmer) at a heating rate of 10 K/min. Thermograms obtained in the second run are shown in Figure 2. Taking as the glass transition temperature the intersection of the baseline of the glassy region with the tangent to the endotherm in the middle point, the values of T_g for DCMMS and DCMS were 212 and 223 K, respectively.
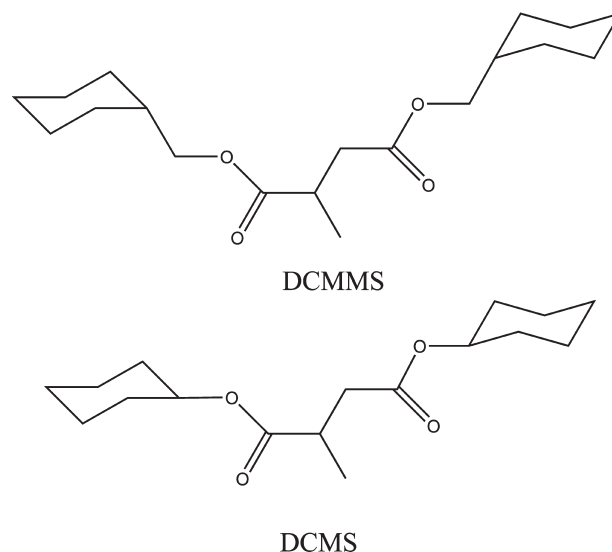

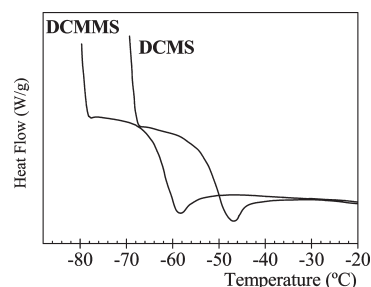**Figure 1.** Schematic structures of DCMMS and DCMS.

Figure 2. DSC thermograms corresponding to the DCMMS and DCMS liquids.

Dielectric experiments were performed in a liquid parallel plate sample cell (BDS1308). The electrode gap was adjusted by silica spacers. The measurements were carried out in the temperature range from −120 to +30 °C and a frequency window of 4.9×10^{-2} to 3×10^6 Hz using a Novocontrol BDS system comprising a frequency response analyzer (Solartron Schlumberger FRA 1260) and a broad-band dielectric converter with an active sample head.

■ RESULTS

Three representative isochrones at 1.19, 95.24, and 11 349 Hz showing the variation of the real (ε') and loss (ε'') components of the complex dielectric permittivity (ε^*) with temperature for DCMMS and DCMS are presented in Figure 3. In order of increasing temperature, the loss isochrone for DCMMS, at 1.19 Hz, exhibits two weak relaxations, named γ and β, followed by an ostensible absorption corresponding to the glass−liquid or α relaxation centered at 213 K. The α relaxation of DCMS is centered at 219 K, ca. 6 K above that of DCMMS. As in the case of DCMMS, the isochrones of DCMS also present the β absorption as a shoulder of the glass−liquid relaxation whereas the γ absorption is not detected in the isochrones.

The ε' isochrones for DCMMS and DCMS slightly increase with temperature in the glassy state. However, as usual, ε' undergoes a steep increase at temperatures located in the vicinity of the glass transition temperature, reaching a pseudoplateau (the maximum value is observed followed by a slight decrease in ε').
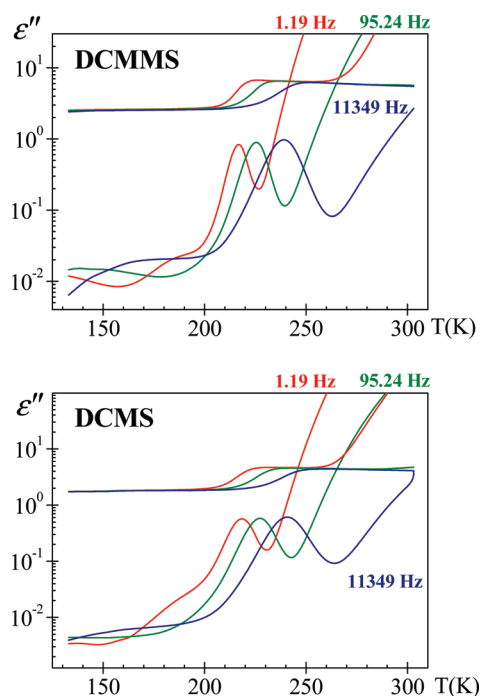
Figure 3. Real and loss components of the complex dielectric permittivity as a function of temperature for DCMMS and DCMS at 1.19, 9.52 × 10, and 1.13 × 10^4 Hz.
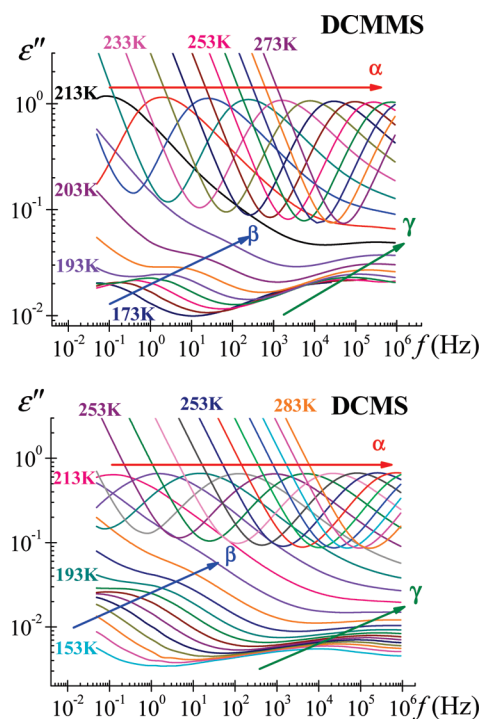

Figure 4. Dielectric loss permittivity as a function of frequency for DCMMS and DCMS in the temperature ranges 173−273 and 153−283 K, respectively (at 5 K steps).

As a consequence of strong electrode polarization (EP) processes, the isochrones at high temperatures depart from the plateau, undergoing a steep increase with increasing temperature.
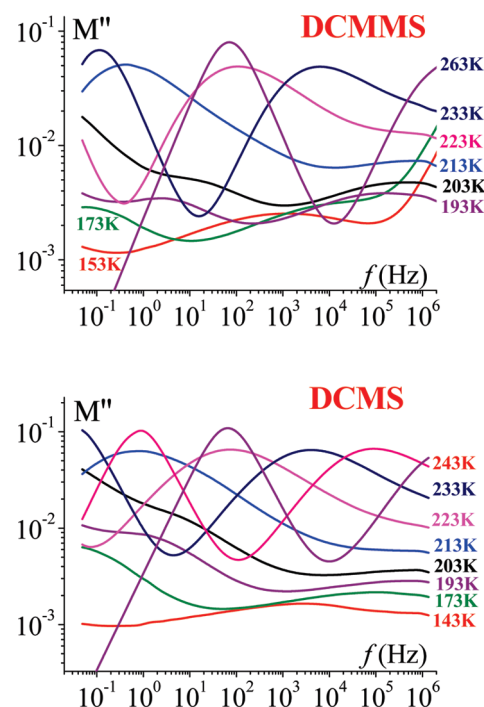

Figure 5. Loss modulus M'' in the frequency domain for DCMMS and DCMS at several temperatures.

For the convenience of further analysis and calculations, the dielectric loss was also plotted in the frequency domain, and the pertinent isotherms for the dielectric loss of DCMMS and DCMS are shown in Figure 4. The β relaxation in the glassy compounds is only detectable in the loss isotherms lying in the range 178−198 K for DCMMS and 183−198 K for DCMS. However, γ relaxations for DCMMS and DCMS in the glassy state are detected in the isotherms over a wider range of temperatures. At temperatures above T_g, the isotherms display an ostensible absorption associated with the glass−liquid relaxation, progressively dominated by the conductive contribution as temperature increases. The real component of the complex permittivity in the frequency domain, shown for DCMMS and DCMS in Figure 1S of the Support Information, increases as the frequency decreases, reaching a pseudoplateau. At high temperatures and in the low-frequency region, ε' strongly increases as the frequency decreases. As indicated above, the steep increase of ε' at low frequencies is caused by EP phenomena.

For systems such as DCMMS and DCMS in which charge contributions to the dielectric permittivity are important at low frequencies, it is also convenient to analyze the results in terms of the complex dielectric modulus, a parameter very sensitive to charge transport. The pertinent loss modulus in the frequency domain for DCMMS and DCMS is shown in Figure 5. For both polymers the loss modulus exhibits above T_g an absorption in the high-frequency region associated with the glass−liquid relaxation followed at lower frequencies by a well-defined peak presumably caused by charge transport arising from electrode polarization.

As a consequence of strong EP processes occurring at low frequencies reflected in the sharp increase of ε' with decreasing frequency, tan δ exhibits a peak below that of the glass−rubber liquid relaxation. The pertinent peaks in the frequency domain are plotted at several temperatures in Figure 6. These results will be used later to
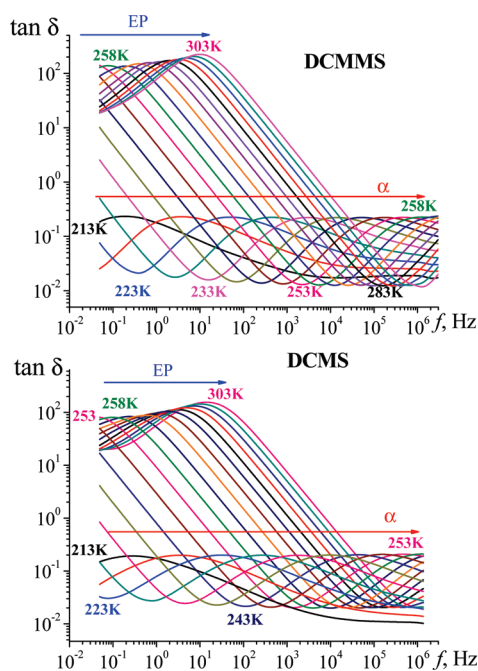
Figure 6. Loss tan δ in the frequency domain for DCMMS and DCMS at 213−303 K (at 5 K steps).

Figure 7. Retardation spectra for DCMMS and DCMS in the temperature ranges 218−253 and 213−248 K, respectively (at 5 K steps). Dashed lines indicate that out of the limits the values of $L(\ln \tau)$ should be regarded as approximate.

model EP processes and thus to obtain information concerning ionic transport at the electrode interfaces.

Deconvolutions of Overlapping Dipolar Relaxations. The complex dielectric permittivity of liquids in the frequency domain, above T_g, is customarily written in terms of Havriliak−Negami (HN)-type equations as

$$\varepsilon^*(\omega) = \varepsilon_\infty + \sum_{k=1}^n \frac{\varepsilon_{0k} - \varepsilon_{\infty k}}{[1 + (j\omega\tau_k)^a]^b} + \left(\frac{\sigma}{je_0\omega}\right)^s \quad (1)$$

where k denotes the type of dipolar relaxation, the subscripts 0 and ∞ refer, respectively, to relaxed ($\omega = 0$) and unrelaxed ($\omega = \infty$) dielectric permittivities corresponding to the relaxation k, τ_k and e_0 are, respectively, the relaxation time associated with the relaxation k and the free space dielectric permittivity, σ is the conductivity arising from charge transport at the liquid−electrode interface, and $s \le 1$ is a parameter that accounts for the departure of the conductive contribution from linearity owing to the interfacial polymer−electrode processes and other phenomena. The shape parameters a and b fulfill the condition $0 < ab \le 1$, and for a Debye process $a = b = 1$.[15] For glasses eq 1 also holds, though in this case the conductivity contribution to the dielectric loss is nil. Deconvolutions are usually carried out by fitting eq 1 to the experimental results.[16] Below T_g eq 1 is also used for deconvolution purposes, making $\sigma = 0$ and $b = 1$.

Retardation time spectra are better defined than dielectric loss spectra in the frequency domain due to the fact that a Debye process is a δ of Dirac in the retardation spectra but it covers 2.29 decades in the loss spectra. Therefore, retardation spectra are more amenable to deconvolution processes of strongly overlapped relaxations. However, owing to strong polarization processes that cause an anomalous enhancement of the dielectric complex permittivity at high temperatures and low frequencies, the computation of retardation spectra and further deconvolution of overlapping relaxations were restricted to the isotherms
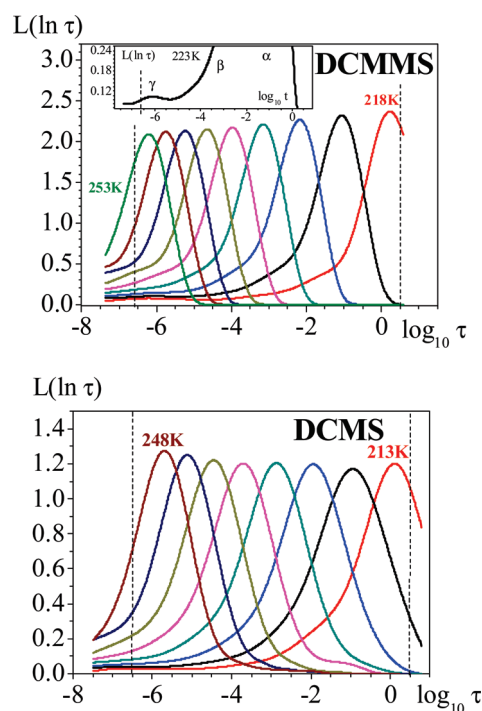
where EP processes are negligible, i.e., 213−253 K for DCMMS and 213−48 K for DCMS. The calculation of retardation spectra can be performed in an efficient way by minimization methods. Briefly, the complex dielectric permittivity is expressed in terms of the retardation spectrum $L(\ln \tau)$ by[17,18]

$$\varepsilon^*(\omega) = \varepsilon_\infty + \int_{-\infty}^{\infty} \frac{L(\ln \tau)}{1 + j\omega\tau} \, d \ln \tau + \left(\frac{\sigma}{je_0\omega}\right)^s \quad (2)$$

This expression can approximately be written in discrete form as

$$\varepsilon^*(\omega_i) = \varepsilon_\infty + \sum_{k=1}^N R_{ik}^* L_k + \left(\frac{\sigma}{je_0\omega}\right)^s \quad (3)$$

where

$$R_{ik}^* = \frac{\Delta \ln \tau_{ik}}{1 + j\omega_i\tau_{ik}} \quad (4)$$

and $\mathbf{L} = \text{col}[L_1(\ln \tau_1), L_2(\ln \tau_2), ..., L_{N-1}(\ln \tau_{N-1}), L_N(\ln \tau_N)]$, L_k being the value of the retardation spectrum at the retardation time τ_k. The components of L_k can be obtained from the minimization of the error function[19,20]

$$E = \sum_{i=1}^n \left\{ \varepsilon^*(\omega_i) - \left[\varepsilon_\infty + \sum_{k=1}^N R_{ik}^* L_k\right] + \left(\frac{\sigma}{je_0\omega}\right)^s \right\}^2 \quad (5)$$

Owing to the ill-conditioned behavior of eq 5, the Tikhonov regularization technique[21,22] was used to minimize E, and the pertinent steps to carry out this task that lead to the evaluation of L are described in detail elsewhere.[20] Retardation spectra above and below the glass transition temperatures are presented in
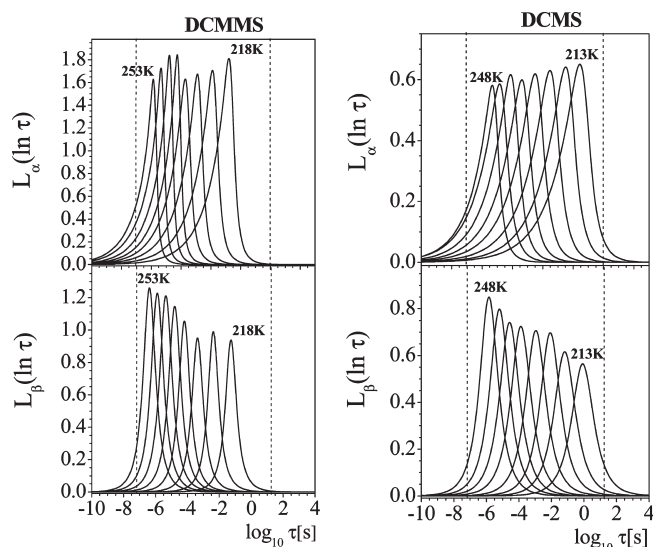
Figure 8. Retardation spectra for DCMMS (218−253 K, 5 K steps) and DCMS (213−248 K, 5 K steps) corresponding to α and β processes. Dashed lines indicate that out of the limits the values of $L(\ln \tau)$ should be regarded as approximate.

Figure 9. Reconstruction of the dielectric loss from the distribution of retardation times for DCMMS and DCMS at several temperatures. Open circles represent the experimental data, and the continuous line represents the dielectric loss calculated as the sum of the individual processes. Inset: relative error calculated as $(\varepsilon_{calcd} - \varepsilon_{exptl})/\varepsilon_{exptl}$.

Figure 7. Below T_g, the spectra for DCMMS and DCMS exhibit two processes corresponding in increasing order of time to the γ and β relaxations. Above T_g, the secondary β absorption strongly overlaps with the prominent glass−liquid relaxation in the two models. The γ absorption above T_g was only detected in DCMMS.

Deconvolutions of the overlapped relaxations were carried out using the analytical forms of retardation spectra corresponding to HN-type equations by using the procedures described elsewhere,[20,23,24] and the pertinent spectra for the individual relaxations of DCMMS and DCMS are shown in Figure 8. To test the reliability of the deconvolutions of the retardation spectra, the strengths of the individual relaxations were calculated by means of the following expression:

$$\varepsilon_{0k} - \varepsilon_{\infty k} = \Delta\varepsilon_k = \int_{-\infty}^{\infty} L_k(\ln \tau) \, d \ln \tau \qquad (6)$$

where k denotes the relaxation, γ, β, or α. The relative error of the difference between the sum of the strengths of the relaxation and that of the overall spectrum, i.e., $(\varepsilon_0 - \varepsilon_{\infty} - \sum_{k=1}^{n}\Delta\varepsilon_k)/(\varepsilon_0 - \varepsilon_{\infty})$, is in the most unfavorable case less than 2%. The strengths and shape parameters of the deconvoluted relaxations were used in eq 1 to recalculate the dielectric loss of DCMMS and DCMS in the frequency domain, and the results obtained (continuous lines) together with the relative errors are shown in Figure 9. It is worth noting that for most frequencies the relative error involved in the calculations lies below 5%. As an example, the deconvolution of the retardation time spectrum for DCMMS at 223 K is plotted in Figure 2S of the Supporting Information. It can be seen that the fitting requires postulation of the existence of three peaks named in increasing order of time γ, β, and α.

Below T_g, deconvolutions of the γ and β processes of DCMMS and DCMS were also carried out directly in the loss spectra by means of eq 1 using $b = 1$ and $\sigma = 0$. In general, the strength and shape parameters were in excellent agreement with those obtained from the retardation spectra. As occurs in the dielectric loss spectra, the β relaxation in the retardation time
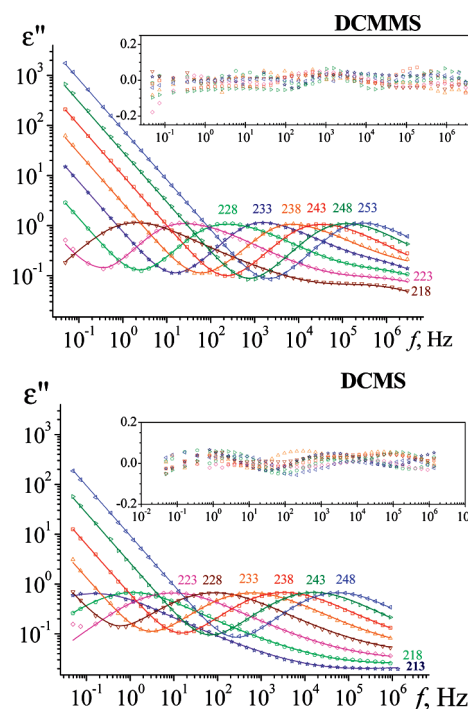
spectra is only detectable in the temperature range of 178−198 K for DCMMS and 183−198 K for DCMS. However, the γ relaxation of DCMMS in the glassy state appears in a rather wide range of temperatures.

Values of the strengths of the glass−liquid and secondary relaxations of DCMS and DCMMS are shown in Figure 10. In general, the strengths of the fast relaxations, γ and β, increase with increasing temperature in the glassy state, the β relaxation undergoing a steep augment in the glass liquid transition. In the liquid state, the strength of the β relaxation moderately increases with increasing temperature. However, as usual, the strength of the α relaxation decreases with increasing temperature as a consequence of the fact that the thermal energy disturbs the alignment of the dipole of the molecules intervening in the cooperative motions that give rise to the relaxation. Moreover, in general, the strengths of the secondary and glass−liquid relaxations for DCMMS are somewhat larger than those computed for DCMS.

The shape parameters of the relaxations are plotted as a function of temperature in Figure 11. It should be remembered that the shape parameter a accounts for the departure of the relaxation from a semicircle in the complex ε' vs ε'' plots whereas the parameter b is associated with the skewness of the plots at high frequencies in the case of the glass−liquid relaxation. The values of a for the β relaxation of DCMMS are somewhat lower than those corresponding to the α relaxation. In general, $a_\gamma < a_\beta < a_\alpha$. Although the departure of the α relaxation from a semicircumference is rather small at low frequencies, the low value of b indicates a strong skewness of the complex plots at high frequencies. In general, the values of the shape parameters for DCMS, shown in Figure 11, are somewhat lower than those obtained for DCMMS.
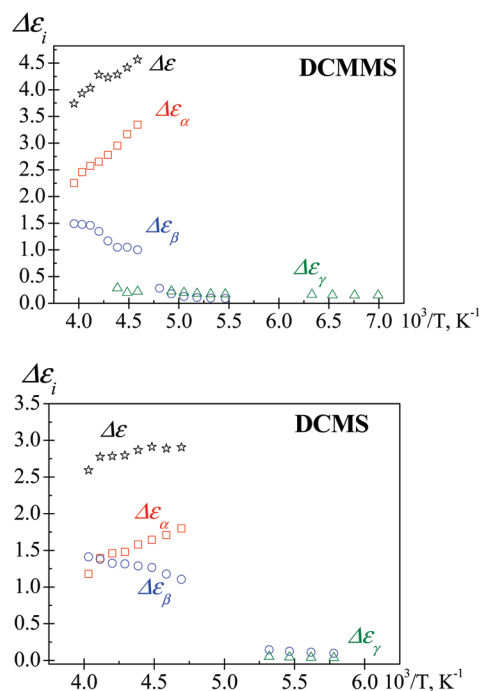
5734

dx.doi.org/10.1021/jp110554h |*J. Phys. Chem. B* 2011, 115, 5730–5740

Figure 10. Temperature dependence of the strengths of the α (open squares), β (open circles), and γ (open triangles) relaxations for DCMMS and DCMS. Black stars represent the total dielectric strength.
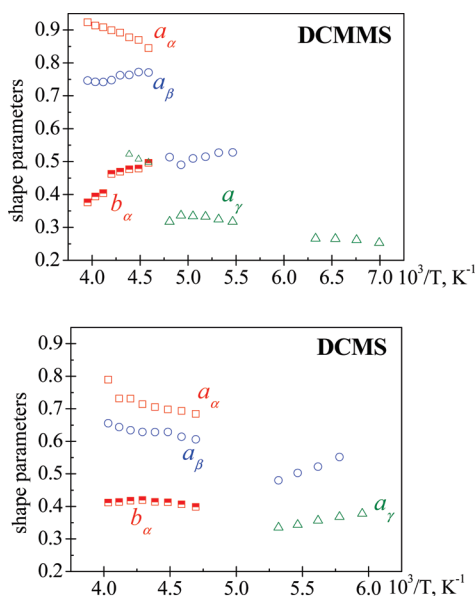

Figure 11. Temperature dependence of the shape parameters of the α (open squares), β (open circles), and γ (open triangles) relaxations for DCMMS and DCMS.

■ DISCUSSION

In spite of the similarity of the structures of DCMMS and DCMS, the former compound has a T_g about 10 K below that of the latter. The cause of this difference lies in that the methylene group separating the oxygen of the ester residue from the cyclohexyl group increases the flexibility and the conformational entropy of DCMMS. However, the T_g of the molecular compounds is dependent not only
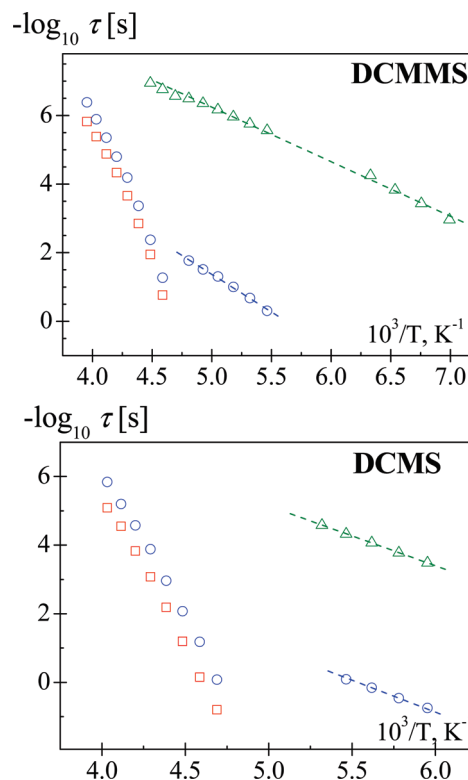

Figure 12. Arrhenius plots for the α (squares), β (circles), and γ (triangles) relaxations for DCMMS and DCMS.

on the molecular flexibility but also on the intermolecular interactions, especially those arising from dipole—dipole interactions that tend to increase the glass transition temperature. These interactions may be higher in DCMS than in DCMMS. Actually, in the *all-trans* conformation the dipoles associated with the ester groups of both molecules are nearly in the parallel direction, and hence, this conformation has the highest polarity. Departure from the *trans* conformation, and therefore a decrease in the polarity of the molecule as a whole, is more probable in the case in which the relatively bulky cyclohexyl moiety is separated from the rest of the molecule by a methylene group as occurs in DCMMS. As a result, intermolecular dipole—dipole interactions may be stronger in DCMS than in DCMMS. Motions associated with intramolecular transitions in the cyclohexyl ring presumably cause the γ process detected in the models. The origin of the β relaxation will be discussed later on.

As indicated above, the analysis of the temperature dependence of the relaxations was restricted to the temperatures at which EP processes are negligible, and the pertinent Arrhenius plots for the different relaxations are shown in Figure 12. As usual, the variation of the relaxation time with temperature for the glass—liquid relaxation is described by the Vogel—Fulcher—Tammann—Hesse (VFTH) equation

$$\tau(T) = \tau_0 \exp[D_0 T_V/(T - T_V)] \tag{7}$$

where τ_0 is a prefactor on the order of picoseconds and D_0 and T_V are, respectively, the fragility parameter and the Vogel temperature. The VFTH fitting parameters are collected in Table 1. Notice that the fragility parameter is smaller than 10, the frontier that separates fragile glasses ($D_0 < 10$) from strong ones ($D_0 > 10$).[1,25]

Table 1. Activation Energies of the Secondary Relaxation and Parameters of the VFTH Equation [$\tau = \tau_0 \exp[D_0/(T/T_V - 1)]$] for DCMMS and DCMS

sample		DCMMS	DCMS
$E_{a,\gamma}$ (kJ·kmol^{-1})		30.6 ± 0.5	30.1 ± 0.8
$E_{a,\beta}$ (kJ·mol^{-1})		40.1 ± 0.7	35.0 ± 0.8
α	D_0	8.86 ± 1.81	7.89 ± 1.17
	T_V (K)	164 ± 2	173 ± 2
	ϕ_g/B (%)	3.3 ± 0.4	3.7 ± 0.6
	$\alpha_f \times 10^4$ (K^{-1})	6.88 ± 1.21	7.32 ± 1.31
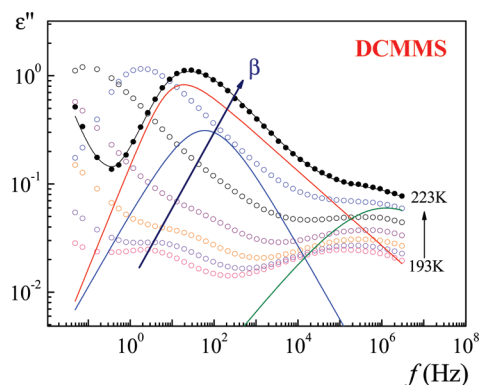
Figure 13. Dielectric loss permittivity for DCMMS in the frequency domain and temperature range 193–223 K. For illustrative purposes, the deconvolution of the relaxations at 223 K is shown. The red line represents the α relaxation, the blue line the β process, and the green line the γ relaxation. The black line represents the dielectric loss permittivity recalculated from the deconvoluted relaxations.

By comparing the VFTH equation with the Doolitle equation[26]

$$\tau = \tau_0 \exp(B/\Phi) \tag{8}$$

where Φ is the relative free volume and B is a parameter close to unity, it is found that the relative free volume and the expansion coefficient of the free volume α_f at T_g are given by

$$\Phi_g/B = (T_g - T_V)/D_0 T_V$$
$$\alpha_f = (1/V)(\partial V/\partial T)_p = 1/(D_0 T_V) \tag{9}$$

The values of Φ_g/B and α_f obtained by means of eq 9 are also collected in Table 1. It is worth noting that the results obtained for the free volume at T_g are slightly higher than the average value of 0.025 ± 0.005 reported for most liquids at the glass transition temperature, independently of the molecular weight, and α_f is somewhat lower than 10^{-3} K^{-1} found for most low molecular weight liquids.[27]

The variation of the relaxation times associated with the β process with temperature, in the glassy state, is shown in Figure 12. It can be seen that the relaxation follows Arrhenius behavior with activation energies of 40.1 and 35.0 kJ·mol^{-1} for DCCMS and DCMS, respectively. Moreover, the γ relaxations for DCMMS and DCMS also obey Arrhenius behavior in the glassy state with activation energies of 30.6 and 30.3 kJ·mol^{-1}, respectively. Neither the β nor the γ relaxations are clearly observable in the dielectric loss spectra at $T > T_g$. On the other hand, the well-developed relaxation displayed in the spectra

cannot be fitted by a simple HN-type equation presumably due to the presence of a secondary relaxation hidden by the α relaxation. An excess wing detected in a variety of glass formers is attributed in many cases to the high-frequency side of a β process hidden by the glass liquid relaxation.[28–30] For illustrative purposes, the deconvolution of the loss isotherm of DCMMS at 223 K is shown in detail in Figure 13. The strength and shape parameters used for the deconvolutions were obtained from the deconvolution of the corresponding retardation time isotherm shown in Figure 2S in the Supporting Information. It can be seen that the broad relaxation peak can be deconvoluted into three peaks corresponding in order of increasing frequency to the α, β, and γ relaxations. In Figure 13, the displacement of the location of the β peak maximum with temperature is indicated by an arrow. It is important to point out that the strength of the β process undergoes a sharp increase in passing from the glassy to the liquid state. Moreover, the temperature dependence of the β process at $T > T_g$, shown in Figure 12, is not of Arrhenius type, behaving similarly to the structural relaxation. A sharp increase of the strength of the β process in the glass–liquid transition has been reported for poly(5-acryloxy-5-ethyl-1,3dioxacyclohexene).[31] However, the temperature dependence of the relaxation is of Arrhenius type below and above T_g in this polymer.

It has been argued that the excess wing and β relaxations are different processes corresponding to the existence of two classes of glass formers:[32] type A with an excess wing and type B with a β process. The β process in type B glass formers obeys Arrhenius behavior, while the analysis of the temperature dependence of glass formers of type A reveals significant deviations from the thermally activated process. It had been suspected long ago[33] that in systems without a well-resolved β process the relaxation times of the α and β processes are close together due to an uncommon temperature dependence of the relaxation time associated with the β process. Tanaka[30] considers that the strong coupling between cooperative rotational motion associated with creation and annihilation of metastable islands (α mode) and local rotational jump motion in a cage (slow β mode) appears as the excess wing having the character of the α mode, whereas a strong decoupling case appears as an independent local mode having Arrhenius behavior. According to the unified picture of local orientational fluctuations, the strong coupling between the α and β modes is responsible for the closeness temperature dependences of the α and β relaxations associated with the dynamics of DCMMS and DCMS at temperatures above T_g. The α mode character of the β process at temperatures above T_g for DCMMS and DCMS suggests that the secondary process presumably is produced by coordinate motion of the whole molecule, similarly to that believed to occur in the so-called JG β relaxations. However, intramolecular local motions produce the β relaxation below T_g, which as shown in Figure 12 exhibits Arrhenius behavior.

It is worth noting that the same Arrhenius plot roughly fits the temperature dependence of the γ process above and below T_g. The decoupled β absorptions carried out in the retardation time spectra at $T > T_g$ (Figure 8) are symmetric, in consonance with one of the requirements of second-order relaxations. It is important to point out that the strength of the β process undergoes a sharp increase in passing from the glassy to the liquid state.

Values of the ionic conductivity σ were obtained as a function of temperature by the minimization procedure used to compute the retardation time spectra. The values obtained and their temperature dependence, plotted in Figure 14, show that the ionic conductivity follows Arrhenius behavior with activation
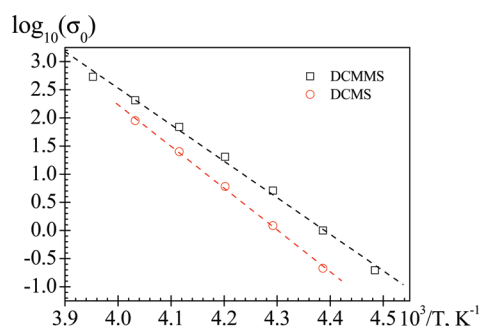
Figure 14. Arrhenius plot showing the temperature dependence of the ionic conductivity ($\Omega^{-1}\,m^{-1}$) for DCMMS (squares) and DCMS (circles). The s parameter was approximately 1 for all temperatures analyzed.

energies of 127.5 and 151.1 kJ·mol^{-1} for DCMMS and DCMS, respectively. The high activation energy associated with the ionic transport process, also observable in the conductivity of some polymers,[34−38] suggests that a relatively high number of molecules are involved in the formation of holes through which the ionic species diffuse. It should be remembered that the ionic transport contributes to the dielectric loss but not to the real component of the complex conductivity.

The departure of DCMMS and DCMS from Arrhenius behavior in the vicinity of T_g can be estimated in terms of the dynamic fragility index, m, that characterizes the rapidity with which the physical properties of a supercooled liquid vary as the temperature approaches the glass transition temperature. The pertinent expression for m is[39,40]

$$m = \lim_{t \to \infty}\left(\frac{d\log\xi}{d(T/T_g)}\right)_P \quad (10)$$

where ξ is a physical parameter, such as the viscosity η or the relaxation time τ, depending on the dynamics of the system. Taking this latter parameter as a reference, the dynamic fragility index can be written as

$$m = \frac{D_0 T_V}{2.303 T_g (1 - T_V/T_g)^2} \quad (11)$$

The value of m for DCMMS ($m = 58.1$) is rather close to, though slightly larger than, that of DCMS ($m = 55.9$). Plots of m vs T_g for different glass formers show a roughly linear increase of the dynamic fragility coefficient with the glass transition temperature. The pertinent expressions that relate m with T_g are $m^* = (0.28 \pm 0.067)(T_g\,(K)) + (9 \pm 20)$ for polymers and monomers and $m^* = (0.25 \pm 0.059)(T_g\,(K)) + (16 \pm 10)$ for hydrogen-bonding organic and inorganic liquids.[40] The values obtained for m^* from these empirical expressions are 68.4 and 70.6 for DCMMS and DCMS, respectively.

The apparent activation energy associated with the α relaxation at T_g can be obtained by equating the fragility indices obtained from VFTH and Arrhenius behavior, i.e.

$$m = \left[\frac{d\log\tau_A}{d\log(T/T_g)}\right]_{T=T_g} = \left[\frac{d\log\tau_{VFTH}}{d\log(T/T_g)}\right]_{T=T_g} \quad (12)$$

Taking into account that $\tau_A = \exp(-E/RT)$, eq 12 leads to the following expression for the activation energy E_a at T_g:
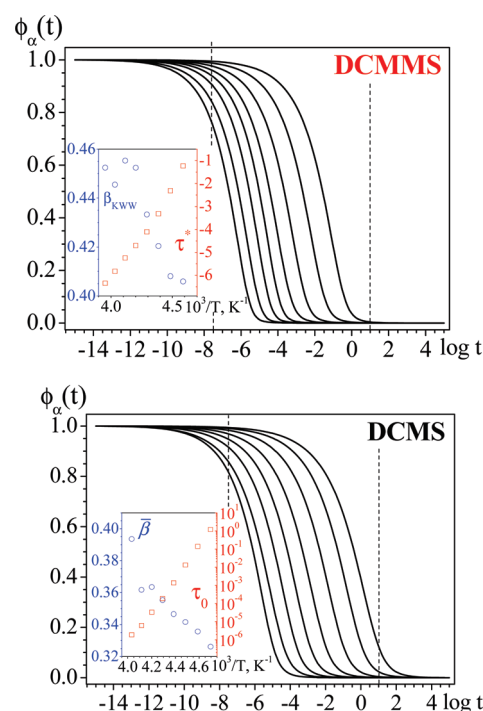

Figure 15. Normalized relaxation curves in the time domain for the α relaxation of DCMMS (218−253 K) and DCMS (213−248 K). The decay curves are fitted by the KWW equation using the stretch exponents β_{KWW} and the characteristic relaxation times τ^* shown in the inset of the figure. Dashed lines indicate that out of the limits the values of $\phi(t)$ should be regarded as approximate.

$$E_a(T_g) = \frac{R D_0 T_V}{(1 - T_V/T_g)^2} \quad (13)$$

From eqs 11 and 13, the activation energy can be expressed by the alternative form

$$E_a(T_g) = 2.303 R m T_g \quad (14)$$

Accordingly, the higher the T_g, the higher the activation energy (under constant pressure and volume). The values of the activation energies of DCMMS and DCMS at T_g are, respectively, 235.7 and 231.5 kJ·mol^{-1}. These results are in rather good agreement with those calculated from the empirical relationship $E_a(T_g)\,(kJ\cdot mol^{-1}) = [0.006(T_g\,(K))^2 - 35]$,[40] which gives 235.3 and 255.4 kJ·mol^{-1}.

The normalized glass−liquid relaxation in the time domain $\phi(t)$ can be obtained from the retardation spectra by

$$\phi(t) = \frac{\int_{-\infty}^{\infty} L_\alpha(\ln\tau)e^{-t/\tau}\,d\ln\tau}{\int_{-\infty}^{\infty} L_\alpha(\ln\tau)\,d\ln\tau} \quad (15)$$

where L_α is the retardation spectrum corresponding to the α relaxation. The pertinent functions in the time domain for DCMS and DCMMS are shown in Figure 15. As usual, decay glass−liquid relaxations are described by the Kohlrausch−Williams−Watts (KWW) equation[10]

$$\phi(t) = \exp[-(t/\tau^*)^{\beta_{KWW}}] \quad (16)$$

where the stretch exponent β_{KWW} lies in the range $0 < \beta_{KWW} \leq 1$ and τ^* is a characteristic relaxation time. The dependence of the KWW parameters on temperature is shown in the inset of Figure 15. It can be seen that for DCMS β_{KWW} increases with temperature from 0.33 at 213 K to 0.39 at 248 K whereas for DCMMS this parameter increases from 0.41 at 213 K to 0.45 at 248 K. The results obtained for the stretch exponent of the α relaxation of these monomers lie in the same range as those reported for polymers. Therefore, the complexity of the cooperative motions in low molecular weight liquids is apparently similar to that found for high molecular weight rubbery liquids.

The increase observed in ε' with decreasing frequency after this parameter reaches the plateau arises from either interfacial polarization and/or EP. The EP process proceeds from charge accumulation at the electrode–polymer interfaces, whereas the interfacial polarization is due to buildup of charges at the interfaces of components of heterogeneous systems.[41] The contribution to the dielectric loss in EP processes scales as ω^{-s}, where s is a parameter close to unity, but the interfacial polarization in the bulk manifests itself as a Maxwell–Wagner–Sillars (MWS) relaxation[42−44] produced by transport of charges separated over a considerable distance with respect to the atomic or segment size. It is worth noting that segregation of hydrophilic moieties from hydrophobic ones in otherwise homogeneous systems may give rise to distributed MWS relaxations produced by a variety of environments,[34] reflected by an α' peak for some systems located in the retardation peaks at longer times than the glass–rubber (α) relaxation. The α' peak is nearly negligible in the retardation spectra of DCMMS and DCMS, this fact ruling out a substantial contribution of interfacial polarizations in the bulk to the relaxation behavior of these compounds at low frequencies. Therefore, EP processes govern the responses of DCMMS and DCMS in the liquid state to low-frequency electric perturbation fields. Although the exact nature of the impurities that produce EP phenomena is unknown, ions coming from dissociation of traces of water as well as ionic impurities contained by the solvents and chemical compounds used in the synthesis of the model compounds may be responsible for the electrode polarization at low frequencies.

Long ago MacDonald[45] and Coelho[46] viewed EP processes as a result of the relaxations of macrodipoles produced by charges located near the polymer–electrode boundary. The orientation of the macrodipole goes from the positive to the negative electrode, and at low frequency, it follows the field, giving rise to a polarization process. Modeling the sinusoidal application of an electric field, the EP process can be represented by a simple Debye relaxation[46,47] (for details see the Supporting Information):

$$\varepsilon^*_{EP} = \varepsilon_R + \frac{\Delta\varepsilon_P}{1 + j\omega\tau_{EP}} \tag{17}$$

where $\Delta\varepsilon_{EP} = \varepsilon_{R,EP} - \varepsilon_R$, ε_R being the relaxed dipolar dielectric permittivity. Moreover, $\varepsilon_{R,EP} = \varepsilon_R L/2L_D$, where L_D and L are, respectively, the Debye length and the thickness of the material sandwiched between the electrodes. According to the theory, the loss tan δ peak appearing at low frequencies is given by

$$\tan\delta = \frac{\omega\tau_{EP}}{1 + \omega^2\tau_{EP}^2(2L_D/L)} \tag{18}$$

where

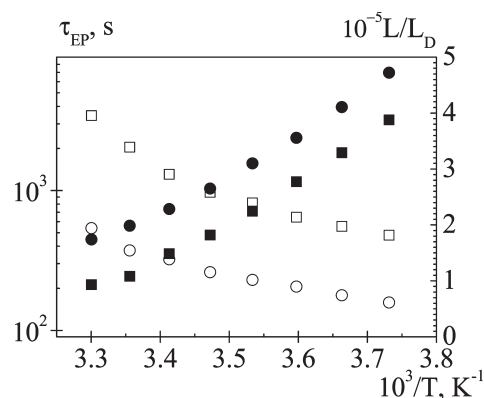$$\tau_{EP} = \frac{LF}{2\sigma}\left(\frac{\varepsilon_0\varepsilon_R I}{k_B T}\right)^{1/2} \tag{19}$$

Figure 16. Temperature dependence of τ_{EP} (s) (full symbols) and L/L_D (open symbols) for DCMMS (squares) and DCMS (circles).

In this expression $I = \sum_i z_i^2 c_i$ is the ionic strength, z_i and c_i being, respectively, the concentration and valence of the ionic species i. The frequency at the peak maximum, Ω_{max}, is given by

$$\Omega_{max} = \frac{(L/2L_D)^{1/2}}{\tau_{EP}} = \frac{1}{(\tau\tau_{EP})^{1/2}} \tag{20}$$

and tan δ at the peak maximum can be written as

$$\tan\delta_{max} = \frac{1}{2}\left(\frac{L}{2L_D}\right)^{1/2} \tag{21}$$

From eqs 20 and 21 the relaxation time τ_{EP} and the Debye length L_D can be calculated, i.e., from the values of tan δ_{max} and Ω_{max} obtained from Figure 6. The temperature dependences of τ_{EP} and L_D are shown in Figure 16. Taking into account that the liquid thickness is 0.1 mm and the ratio L/L_D is on the order of 10^{-5}, the value of the Debye length is about 1 nm. The results of Figure 16 show that L_D is somewhat higher for DCMMS than for DCMS and in both cases the Debye length slightly decreases with increasing temperature. In the calculation of the Debye length in polymers using the Trukhan method, similar behavior is observed.[48,49] Strictly speaking, with increasing temperature the thermal energy is augmented and disruption of the atmospheres surrounding the ions occurs; as a result, the Debye length should increase. Augmentation of the Debye length with increasing temperature is observed in very dilute electrolyte solutions.[50] The temperature dependence of τ_{EP} is described by the VFTH equation, and the values obtained for $D_0 T_V$ for DCMMS and DCMS are 1150 and 1060, respectively, T_V having the same values as those found for the glass–liquid relaxation. Accordingly, the relative free volume at T_g expressed in terms of Φ_g/B is 0.042 and 0.047 for DCMMS and DCMS, respectively, ca. 1.27 times the values of Φ_g/B obtained from the temperature dependence of the glass–liquid relaxation. Accordingly, the ratio between the critical volume and the volume of the segments involved in the relaxation is somewhat higher in ionic transport relaxation than in the glass–liquid process.

To estimate the values of the concentration and diffusion coefficients of ionic species, it is necessary to know their chemical nature. Unfortunately, this characteristic is not known, but to get a glimpse of the magnitude of these quantities, it will be assumed that a monovalent 1:1 electrolyte is responsible for the EP processes. The relaxation time τ_{EP} and the conductivity σ_0 (the real component of the complex conductivity independent of the frequency) are related
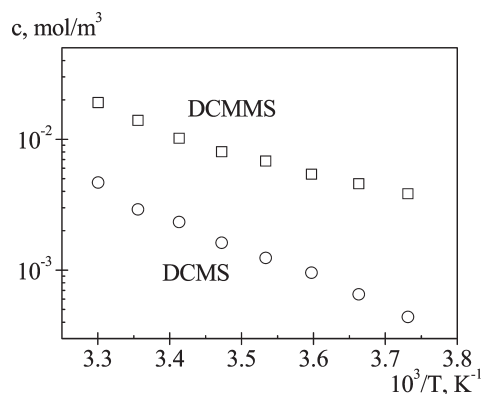
Figure 17. Concentration of ionic species vs reciprocal of temperature for DCMMS (squares) and DCMS (circles).
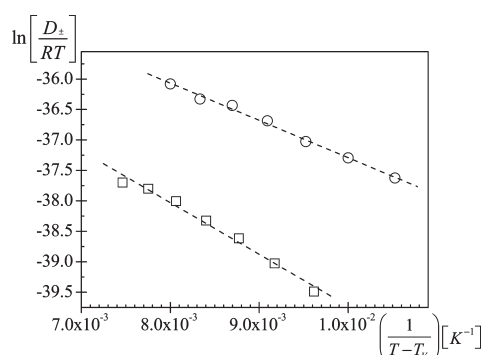

Figure 18. Temperature dependence of the geometric average diffusion coefficient of ionic species for DCMMS (squares) and DCMS (circles).

to the concentration and mobility μ of the ionic species by the expressions $\sigma_0 = Fc(\mu_+ + \mu_-)$ and $\tau_{EP} = (LF/2\sigma_0)(2e_0\varepsilon_R c/k_B T)^{1/2}$ (see the Supporting Information). In these expressions, F is the Faraday constant and e_0 and ε_R are, respectively, the permittivity in the empty space and the relaxed dipolar dielectric permittivity (see eqs7 and 9 of the Supporting Information). In these expressions, ε_R was estimated by fitting eq 17 to the high-frequency side of the experimental curves of ε'_{EP}. The results obtained, collected in Figure 17, show that the concentration of ionic species in DCMMS is nearly 1 decade above that in DCMS. Moreover, the fact that the concentration increases with increasing temperature suggests that the ionic species are trapped in the bulk in such a way that their visibility in transport depends on the mobility of the molecules of the samples.

Taking into account the relationship between ionic mobility and ionic diffusion ($\mu_i = FD_i/RT$), the geometric average of the diffusion coefficient of the ionic species, $D_\pm = (D_+ D_-)^{1/2}$, can be written as

$$D_\pm = \frac{RT\sigma_0}{Fc} \qquad (22)$$

The results for $D_\pm$ at different temperatures are shown in Figure 18. In the temperature range 268–303 K, $D_\pm$ increases from 3.2×10^{-14} to 2.2×10^{-13} m²/s for DCMMS and from 2.0×10^{-14} to 9.6×10^{-13} m²s⁻¹ for DCMS. In the vicinity of T_g, $D_\pm$ depends on the volume and indirectly on temperature in such a way that the friction coefficient that accounts for the interactions between the diffusing species and the surroundings can be expressed in terms of the empirical Doolittle equation $\chi = \chi_0 \exp(-B/\Phi)$, where Φ is the relative free volume and B a parameter

close to unity. By taking into account Einstein's relationship between χ and $D_\pm$, it is found that

$$D_\pm = RTD'_0 \exp\left(\frac{-B}{T - T_V}\right) \qquad (23)$$

where the pre-exponential factor D'_0 is the reciprocal of χ_0 (mol kg⁻¹ s) and B is a constant. Unfortunately, the data we dispose do not correspond to temperatures near T_g where the volume effects are more important. However, the available data suggest that the ratio between the critical volume for a diffusive step and the volume of the segments involved in the formation of the critical volume is somewhat higher for DCMMS than for DCMS.

■ CONCLUSIONS

The two additional methylene groups in bis(cyclohexylmethyl) 2-methylsuccinate with respect to dicyclohexyl 2-methylsuccinate increase the conformational versatility of the former compound, shifting the location of the glass—liquid relaxation to lower frequencies. The two methylene groups also increase the probability of conformations in which the dipoles associated with the ester groups are in the parallel direction, thus increasing the dielectric strength of the glass—liquid relaxation of DCMMS with respect to that of DCMS.

The strength of the β relaxation of DCMMS and DCMS exhibits a sharp increase in the transition from the glassy to the liquid state. Moreover, in the glassy state the β process behaves as a fast relaxation of intramolecular origin that obeys Arrhenius behavior, while in the liquid state it becomes a slower relaxation whose temperature dependence is similar to that of the glass—liquid relaxation. The β relaxation in the liquid state may be provoked by coordinated motions of the whole molecule. The same Arrhenius plot fits the temperature dependence of the γ relaxation of DCMMS in the liquid and glassy states.

The spectra of the two compounds expressed in terms of the loss tan δ also exhibit a relaxation at lower frequency than the glass—liquid relaxation presumably caused by the motion of macrodipoles arising from the concentration of charges in the electrode—liquid interfaces. The analysis of this relaxation expressed in terms of loss tan δ and a single relaxation time in conjunction with Nernst electrochemical type equations allows the rough estimation of the charge concentration and diffusion coefficients.

■ ASSOCIATED CONTENT

ⓢ Supporting Information. Figure showing the frequency dependence of the real component of the dielectric complex permittivity at several temperatures for DCMMS and DCMS, details of the procedure for deconvolution of the retardation spectra and, as an example, a figure with the deconvolutions of the α, β, and γ relaxations in the retardation time isotherm of DCMMS, at 233 K, and details of the modeling of ionic transport employed in the characterization of the EP process. This material is available free of charge via the Internet at http://pubs.acs.org.

■ AUTHOR INFORMATION

Corresponding Author
*E-mail: rdiazc@ter.upv.es (R.D.-C.); riande@ictp.csic.es (E.R.). Phone: 34-96-3879324 (R.D.-C.); 34-91-5622900 (E.R.). Fax: 34-96-3877329 (R.D.-C.); 34-91-5644853 (E.R.).

5739

dx.doi.org/10.1021/jp110554h |*J. Phys. Chem. B* 2011, 115, 5730–5740

■ REFERENCES

(1) Angell, C. A. *Science* **1995**, *267*, 1935.

(2) Donth, E. *Relaxations and Thermodynamics in Polymers: Glass Transition*; Akademie: Berlin, 1992.

(3) Lukenheimer, P.; Schneider, U.; Brand, R.; Lidl, A. *Contemp. Phys.* **2000**, *41*, 15.

(4) Hodge, I. M. *J. Non-Cryst. Solids* **1994**, *169*, 211–266.

(5) Hutchinson, J. M. *Prog. Polym. Sci.* **1995**, *20*, 703–760.

(6) Williams, G. *Macromol. Symp.* **2009**, *286*, 1.

(7) Mpoukouvalas, K.; Floudas, G.; Williams, G. *Macromolecules* **2009**, *42*, 4690.

(8) Stillinger, F. F. *Science* **1995**, *267*, 1924.

(9) Williams, G. *Trans. Faraday Soc.* **1966**, *62*, 2091.

(10) Williams, G. *Adv. Polym. Sci.* **1979**, *39*, 59.

(11) Johari, G. P.; Goldstein, M. *J. Chem. Phys.* **1970**, *53*, 2372.

(12) Johari, G. P. *Ann. N. Y. Acad. Sci.* **1976**, *279*, 117.

(13) Williams, G. In *Keynote Lectures in Selected Topics of Polymer Science*; Riande, E., Ed.; Consejo Superior de Investigaciones Científicas: Madrid, 1995; Chapter 1.

(14) Riande, E.; Saiz, E. *Dipole Moments and Birefringence of Polymers*; Prentice Hall: Englewood Cliffs, NJ, 1992; Chapter 4.

(15) Havriliak, S.; Havriliak, S. J. *Dielectric and Mechanical Relaxation in Materials*; Hanser: Munich, 1997.

(16) Richert, R. *J. Phys.: Condens. Matter* **2002**, *14*, R703–R738.

(17) McCrum, N. G.; Read, B. E.; Williams, G. *Anelastic and Dielectric Effects in Polymeric Solids*; Wiley: London, 1967; Chapter 4.

(18) Riande, E.; Díaz-Calleja, R. *Electrical Properties of Polymers*; Dekker: New York, 2004.

(19) Álvarez, C.; Lorenzo, V.; Riande, E. *J. Chem. Phys.* **2005**, *122*, 194905.

(20) Domínguez-Espinosa, G.; Ginestar, D; Sanchis, M. J.; Díaz-Calleja, R.; Riande, E. *J. Chem. Phys.* **2008**, *129*, 104513. The program employed in the determination of the retardation spectra is available in the supporting information of this reference.

(21) Press, W. H.; Teukolsky, S. A.; Vetterling, W. T.; Flannery, B. P. *The Art of Scientific Computing*, 2nd ed.; Cambridge University Press: New York, 1992; Chapter 18.

(22) Morozov, V. A. *Methods for Solving Incorrectly Posed Problems*; Springer: New York, 1984.

(23) Havriliak, S.; Negami, S. *J. Polym. Sci.: Polym. Symp.* **1966**, *14*, 99.

(24) Zorn, R. *J. Polym. Sci., Part B: Polym. Phys.* **1999**, *37*, 1043.

(25) Angell, C. A. In *Complex Behavior of Glassy Systems*, Proceedings of the XIV Sitges Conference, Sitges, Barcelona, Spain, June 10–14, 1996; Rubi, M., Pérez-Vicente, C., Eds.; Springer: Berlin, 1997.

(26) Doolittle, A. K. *J. Appl. Phys.* **1951**, *22*, 1471; **1952**, *23*, 236.

(27) Ferry, J. D. *Viscoelastic Properties of Polymers*, 2nd ed.; John Wiley & Sons Inc.: New York, 1961.

(28) Schneider, U.; Brand, R.; Lunkenheimer, P.; Loidl, A. *Phys. Rev. Lett.* **2000**, *84*, 5560 and references therein.

(29) Pronin, A. A.; Kondrin, M. V.; Lyapin, A. G.; Brazhkin, V. V.; Volkov, A. A.; Lunkenheimer, P.; Loidl, A. *Phys. Rev. E* **2010**, *81*, 041503.

(30) Tanaka, H. *Phys. Rev. E* **2004**, *69*, 021502.

(31) Alvarez, C.; Lorenzo, V.; Riande, E. *J. Chem. Phys.* **2005**, *122*, 194905.

(32) Kudlik, A.; Benkhof, S.; Blochowicz, T.; Tschirwitz, C.; Rössler, E. *J. Mol. Struct.* **1999**, *479*, 201.

(33) Johari, G. P.; Goldstein, M. *J. Chem. Phys.* **1970**, *53*, 2372.

(34) Sanchis, M. J.; Carsí, M.; Ortiz-Serna, P.; Domínguez-Espinosa, G.; Díaz-Calleja, R.; Riande, E.; Alegría, L.; Gargallo, L.; Radic, D. *Macromolecules* **2010**, *43*, 5723–5733.

(35) Sanchis, M. J.; Domínguez-Espinosa, G.; Díaz-Calleja, R.; Guzman, J.; Riande, E. *J. Chem. Phys.* **2008**, *129*, 054903.

(36) Domínguez-Espinosa, G.; Díaz-Calleja, R.; Riande, E. *Macromolecules* **2006**, *39*, 5043–5051.

(37) Domínguez-Espinosa, G.; Díaz-Calleja, R.; Riande, E.; Gargallo, L; Radic, D. *Macromolecules* **2006**, *39*, 3071–3080.

(38) Domínguez-Espinosa, G.; Díaz-Calleja, R.; Riande, E.; Gargallo, L; Radic, D. *J. Chem. Phys.* **2005**, *123*, 114904.

(39) Plazek, D.; Ngai, K. L. *Macromolecules* **1991**, *24*, 1222.

(40) Qin, Q.; McKenna, G. *J. Non-Cryst. Solids* **2006**, *352*, 2977.

(41) Satti, G.; McLachlan, D. S. *J. Mater. Sci.* **2007**, *42*, 6477.

(42) Maxwell, J. C. *Electricity and Magnetism*; Clarendon: Oxford, U. K., 1893.

(43) Wagner, K. W. *Arch. Elektrotech. (Berlin)* **1914**, *2*, 371.

(44) Sillars, R. W. *J. Inst. Electr. Eng. [1889-1940]* **1937**, *80*, 378.

(45) Macdonald, J. R. *Phys. Rev.* **1953**, *92*, 4.

(46) Coelho, R. *J. Non-Cryst. Solids* **1991**, *131−133*, 1136.

(47) Klein, R. J.; Zhang, S. H.; Dou, S.; Jones, B. H.; Colby, R. H.; Runt, J. *J. Chem. Phys.* **2006**, *124*, 144903.

(48) Compañ, V.; Sorensen, T. S.; Díaz-Calleja, R.; Riande, E. *J. Appl. Phys.* **1996**, *79*, 403.

(49) Compañ, V.; Guzmán, J.; Díaz-Calleja, R.; Riande, E. *J. Polym. Sci., Part B: Polym. Phys.* **1999**, *37*, 3027.

(50) *Surface Chemistry and Electrochemistry of Membranes*; Sorensen, T. S., Ed.; Marcel Dekker, Inc.: New York, 1999; Chapter 18.